Ras Diffusion Is Sensitive to Plasma Membrane Viscosity

J. Shawn Goodwin, Kimberly R. Drake, Catha L. Remmert, and Anne K. Kenworthy

Departments of Molecular Physiology & Biophysics and Cell & Developmental Biology, Vanderbilt University School of Medicine, Nashville, Tennessee 37232

ABSTRACT The cell surface contains a variety of barriers and obstacles that slow the lateral diffusion of glycosylphosphatidylinositol (GPI)-anchored and transmembrane proteins below the theoretical limit imposed by membrane viscosity. How the diffusion of proteins residing exclusively on the inner leaflet of the plasma membrane is regulated has been largely unexplored. We show here that the diffusion of the small GTPase Ras is sensitive to the viscosity of the plasma membrane. Using confocal fluorescence recovery after photobleaching, we examined the diffusion of green fluorescent protein (GFP)-tagged HRas, NRas, and KRas in COS-7 cells loaded with or depleted of cholesterol, a well-known modulator of membrane bilayer viscosity. In cells loaded with excess cholesterol, the diffusional mobilities of GFP-HRas, GFP-NRas, and GFP-KRas were significantly reduced, paralleling the behavior of the viscosity-sensitive lipid probes $DiIC_{16}$ and $DiIC_{18}$. However, the effects of cholesterol depletion on protein and lipid diffusion in cell membranes were highly dependent on the depletion method used. Cholesterol depletion with methyl-β-cyclodextrin slowed Ras diffusion by a viscosity-independent mechanism, whereas overnight cholesterol depletion slightly increased both protein and lipid diffusion. The ability of Ras to sense membrane viscosity may represent a general feature of proteins residing on the cytoplasmic face of the plasma membrane.

INTRODUCTION

Theoretical considerations indicate that membrane viscosity should be an important factor in determining D for a membrane protein within the plane of the bilayer (1). This has rarely been observed in vivo, as D for most proteins in the plasma membranes of cells are 10–100× slower than theoretically predicted and also exhibit low M_f (2,3). The slow and/or anomalous diffusion of these molecules is thought to result from a variety of cellular factors including membrane microdomains, cytoskeletal corrals, protein crowding effects, and transient binding events (4–6).

Until recently, fluorescence recovery after photobleaching (FRAP) and single particle tracking studies have relied on antibody-based probes and focused almost exclusively on the properties of transmembrane and glycosylphosphatidylinositol (GPI)-anchored proteins. In contrast, relatively little is known about the factors that regulate the diffusion of proteins anchored to the cytoplasmic face of the plasma membrane via lipid modifications such as S-acylation, myristoylation, or prenylation (7). These proteins are analogous to GPI-anchored proteins in the sense that they are anchored to the membrane by lipid moieties rather than by a transmembrane domain. This does not necessarily imply that such proteins would exhibit lipid-like diffusion, since many of the barriers to diffusion in cell membranes are thought to reside in or connect to the cytoplasmic face of the membrane (4–6,8,9).

Recent studies using GFP-chimeric proteins have provided the first insights into how protein diffusion on the inner leaflet is regulated. In particular, the diffusional mobility of the small GTPase Ras is the fastest of any membrane protein measured to date (10–12). Localized predominantly to the cytosolic face of the plasma membrane, Ras is anchored to the membrane via a farnesyl moiety in conjunction with either S-acylation (HRas and NRas) or a polybasic domain (KRas) (13,14). These moieties also serve to target each isoform to distinct membrane microdomains. In particular, HRas and NRas associate with cholesterol-sensitive lipid rafts, whereas KRas is found predominantly in nonraft domains (11,15–18). Measurements of the lateral mobility of GFP-tagged Ras or the HRas membrane anchor reveal that a small fraction of molecules are either immobile or exhibit confined diffusion, consistent with the hypothesis that these proteins can be at least transiently confined in membrane microdomains (11,12,19,20). Yet remarkably, the vast majority of Ras molecules undergo extremely rapid lateral diffusion ($\sim$1 $\mu m^2/s$), nearly as fast as lipid probes and significantly faster than other membrane proteins (typically 0.01–0.5 $\mu m^2/s$) (11,12).

Based on these observations, we hypothesized that Ras diffusion may exhibit a lipid-like sensitivity to membrane viscosity. To test this hypothesis, we compared the diffusional mobility of the three major Ras isoforms with the mobility of viscosity-sensitive fluorescent lipid probes, $DiIC_{16}$ and $DiIC_{18}$, as a function of cholesterol concentration within the plasma membrane of COS-7 cells.

MATERIALS AND METHODS

Cells and fluorescent probes

COS-7 cells (ATCC) were maintained in Dulbecco's modified Eagle's medium (DMEM) with 10% fetal calf serum as previously described (12).

Submitted November 3, 2004, and accepted for publication May 17, 2005.

Address reprint requests to Anne K. Kenworthy, E-mail: anne.kenworthy@vanderbilt.edu.

0006-3495/05/08/1398/13 $2.00

doi: 10.1529/biophysj.104.055640

enhanced green fluorescent protein (EGFP)-HRas, EGFP-KRas, and EGFP-NRas were the gift of Mark Philips (21). Transient transfections were performed 16–24 h before an experiment using FuGENE 6 (Roche Diagnostics, Indianapolis, IN). $DiIC_{16}$ (3) (1, 1′ –diahexadecyl-3, 3, 3′, 3′-tetramethylindocarbocyanine perchlorate), $DiIC_{18}$ (1, 1′ –dioctadecyl-3, 3, 3′, 3′-tetramethylindocarbocyanine perchlorate) (obtained as Vybrant DiI cell labeling solution), and 1-(4-trimethylammoniumphenyl)-6-phenyl-1,3,5-hexatriene *p*-toluenesulfonate (TMA-DPH) were from Molecular Probes (Eugene, Oregon). Cells were subjected to loading, depletion, or mock incubations and washed before labeling with 0.3–1.5 μg/ml $DiIC_{16}$ (diluted from an ethanol stock) in serum-free imaging buffer supplemented with 0.1% fatty acid-free bovine serum albumin for 5 min at 22°C or as per the manufacturer's instructions for the Vybrant DiI solution.

Cholesterol modulations and semiquantitative analysis of plasma membrane cholesterol levels

Cells were acutely depleted of cholesterol by washing several times in phenol red-free DMEM supplemented with 0.1% bovine serum albumin and 25 mM HEPES (serum-free imaging buffer), followed by incubation in serum-free imaging buffer supplemented with 10 mM methyl-β-cyclodextrin (MβCD; Sigma-Aldrich, St. Louis, MO) for 30 min at 37°C. As a control, mock-treated cells were incubated for 30 min at 37°C with serum-free imaging buffer. As a second method for cholesterol depletion, cells were grown overnight in DMEM containing 10% lipoprotein-deficient fetal calf serum (LPDS) prepared by standard ultracentrifugation techniques and supplemented with 50 μM compactin (Sigma-Aldrich) plus 50 μM mevalonate (Sigma-Aldrich) overnight before experiments (11,22,23). We found that treatment of cells with compactin at the time of transfection prevented Ras from becoming membrane associated. Therefore, cells were transfected the day of plating and allowed to express the protein for a day before shifting into the depletion media. As a control, cells were incubated overnight in media containing normal fetal calf serum in the presence of vehicle alone.

For acute cholesterol loading, cells were incubated with water-soluble cholesterol (MβCD:cholesterol complexes; Sigma-Aldrich) in serum-free imaging buffer at a final concentration of 10 mM MβCD for 30 min at 37°C. As a second method for cholesterol loading, cells were incubated in 25 μM cholesterol added from an ethanolic stock for 6 h at 37°C (23) or were incubated in vehicle alone as a control. For all treatments, plasma membrane cholesterol levels were quantitated by filipin staining as previously described (12).

Imaging and confocal FRAP

After manipulations of membrane cholesterol levels as described above, cells were washed and mounted in fresh serum-free imaging buffer for FRAP measurements. Fluorescence imaging and confocal FRAP were performed using a Zeiss LSM 510 confocal (Carl Zeiss, Thornwood, NY) as described previously (12). In brief, FRAP measurements were performed with a 40× 1.3 NA Zeiss Plan-Neofluar objective at a digital zoom of 4, a scan speed of 9, and the pinhole set at 1–2 Airy units. Prebleach and postbleach images were acquired using low levels of excitation at 488 nm (EGFP) or 543 nm ($DiIC_{16}$ and $DiIC_{18}$). Photobleaching was performed using 10 scans with the 488 nm laser line at 100% transmission in a rectangular region of interest 4 μm wide. For some experiments, a second FRAP measurement (rebleach) was performed on exactly the same cell and bleach region within ~1 min after the first measurement. All FRAP measurements were performed at 22°C.

Fluorescence recoveries in the bleached region and whole cell were quantitated using the Zeiss LSM software. Effective diffusion coefficients (D) were obtained from the postbleach image series using a program that compares experimental and simulated recoveries into the bleach region (24). M_f was calculated as described, including a correction for the irreversible loss of fluorescence due to the photobleach (12,25). Statistical differences were evaluated in KaleidaGraph (Synergy Software, Reading, PA) using the Student's *t*-test. Control experiments indicate that the kinetics of fluorescence recovery depend on scan speed when the number of bleach iterations was held constant. This effect is likely the result of depletion of Ras and DiI from the area surrounding the bleach region as the result of diffusional exchange during the photobleaching event (26). Thus, the D values we report may be slightly underestimated. For presentation purposes, images were exported in tiff format. Where indicated, prebleach images were averaged using NIH Image.

Because Ras is a peripheral membrane protein, in principle, its fluorescence recovery in FRAP experiments could represent a combination of both lateral diffusion and exchange of the protein on and off the membrane as the result of reversible membrane binding. However, control measurements examining the dependence of recovery kinetics of full-length, GFP-tagged HRas and KRas on the size of the bleach area suggest that the recoveries are dominated by lateral diffusion (11,12,27).

Steady-state fluorescence anisotropy measurements

Steady-state anisotropy measurements of TMA-DPH were made by collecting polarized fluorescence images using a Zeiss LSM 510 confocal microscope with a 40× 1.3 NA objective. After modulation of cellular cholesterol levels as described above, cells were labeled with 2 μm TMA-DPH for 10 min at 37°C (28) and rinsed before visualization. TMA-DPH was excited using multiphoton excitation at 710 nm and fluorescence emission collected using an HP 465/170 band-pass filter. Fluorescence anisotropy, r, was calculated from images obtained by vertically polarized excitation in combination with simultaneous capture of either vertically (VV) or horizontally (VH) polarized emission according to

$$r = (I_{VV} - GI_{VH})/(I_{VV} + 2GI_{VH}), \quad (1)$$

where G is the correction factor for polarization bias in the instrument as described (29). Additional corrections for the large NA of the objective lens (30) were performed as described (29).

RESULTS

The lateral mobilities of GFP-HRas, GFP-NRas, and GFP-KRas are similar to each other and the diffusion of $DiIC_{16}$ under steady-state conditions in COS-7 cells as assessed by confocal FRAP

Previous FRAP studies have shown that the diffusional mobilities of GFP fusions of HRas and KRas are similar to one another under steady-state conditions (11,12). The diffusional mobilities of the two proteins differ, however, in their response to cholesterol depletion as a function of their activation state as a result of their residence within distinct membrane microenvironments (11). To further compare the isoform-specific behavior of the Ras proteins, we expressed GFP-HRas, GFP-NRas, or GFP-KRas in COS-7 cells by transient transfection and compared their diffusional mobility using confocal FRAP. In this assay, GFP fluorescence was photobleached from a strip of plasma membrane 4 μm wide by scanning at high laser power. The subsequent exchange of bleached and nonbleached molecules was monitored at low laser power (Fig. 1 *A*). Under steady-state conditions, the recovery of fluorescence in the bleached region was similar

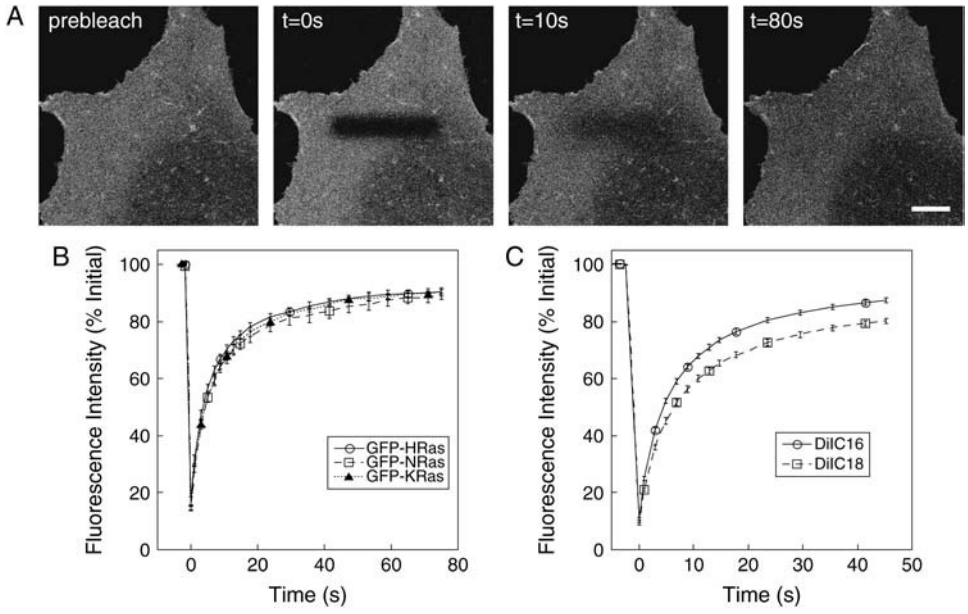

FIGURE 1 Diffusional mobilities of GFP-HRas, GFP-NRas, and GFP-KRas are similar to one another and the fluorescent lipid probes $DiIC_{16}$ and $DiIC_{18}$ in the plasma membrane of COS-7 cells under steady-state conditions as detected by confocal FRAP. (*A*) Example of images collected in a confocal FRAP experiment for GFP-NRas at the indicated times. The bleach strip is 4 μm wide. Postbleach images were acquired every second during the recovery phase. Bar, 10 μm. (*B*) Recovery curves for GFP-HRas (○), GFP-NRas (□), and GFP-KRas (▲) under steady-state conditions. Data shown are from a representative experiment (mean ± SE, $N = 6$–8 cells). (*C*) Recovery curves for $DiIC_{16}$ (○) and $DiIC_{18}$ (□) under steady-state conditions. Data are shown from a representative experiment (mean ± SE, $N = 12$–16 cells). All FRAP data were collected at 22°C at 1 s intervals.

for each protein at 22°C (Fig. 1 *B*). Thus, variations in the membrane anchors among the three Ras isoforms do not substantially alter their average mobility under steady-state conditions, consistent with previous findings (11,12).

To understand the features of cell membranes that regulate Ras diffusion, we first compared its behavior with respect to that of the well-studied fluorescent lipid probes $DiIC_{16}$ and $DiIC_{18}$. Previous work has reported the diffusional mobility of HRas and KRas to be twofold slower than that of $DiIC_{16}$ in Rat-1 cells under control conditions (11). To test whether this is also the case in COS-7 cells, we examined the diffusional mobility of $DiIC_{16}$ and $DiIC_{18}$ (31–33). These probes partition into both liquid-ordered (raft) and liquid-disordered (nonraft) domains (31,33; but see Bacia et al. (34)). Under control conditions, FRAP recoveries were similar for $DiIC_{16}$ and the Ras proteins, whereas the recovery of $DiIC_{18}$ occurred more slowly (Fig. 1, *B* and *C*). Thus, under the conditions of our experiments, the diffusional mobilities of all three Ras isoforms are as fast as or even faster than that of fluorescent lipid probes.

Acute cholesterol depletion and cholesterol loading significantly alter plasma membrane cholesterol levels and the subcellular distribution of both Ras and DiI

Cholesterol is a major modulator of membrane viscosity and also is a key component of lipid rafts, domains with which wild-type HRas is thought to associate (11,14,35). To study the effects of cellular cholesterol levels on the membrane environment sensed by the various Ras isoforms, we used MβCD as a tool to either deplete or load cells with cholesterol (36–38). For depletion experiments, cells were treated with 10 mM MβCD for 30 min at 37°C (12). To increase plasma membrane cholesterol levels, we incubated cells with MβCD/cholesterol complexes for 30 min at 37°C (12). These treatments reduced and increased plasma membrane cholesterol levels to 50% and 300% of control values, respectively, as assessed by filipin staining (Table 1). These two treatments altered cell morphology and the distribution of both the fluorescent lipid probes and Ras in different ways. In particular, MβCD treatment caused the cells to retract and appear smaller (Fig. 2, *F–J*) compared to mock-treated cells (Fig. 2, *A–E*) but had no effect on the subcellular distribution of Ras, $DiIC_{16}$, or $DiIC_{18}$ in the vast majority of the cells examined (Fig. 2, *F–J*). Consistent with a recent report (33), a small fraction of MβCD-treated cells exhibited patchy labeling of $DiIC_{16}$ and $DiIC_{18}$ (data not shown). In striking contrast, cholesterol loading with MβCD/cholesterol complexes lead to an accumulation of $DiIC_{16}$, $DiIC_{18}$, GFP-NRas, and GFP-HRas in patchy and/or vesicular structures (Fig. 2, *K–O*), similar to those observed previously for two different plasma membrane proteins (12).

$DiIC_{16}$ and $DiIC_{18}$ diffusion is unaffected by acute cholesterol depletion, but is slowed in response to acute cholesterol loading

To study the effects of cholesterol loading and depletion on the fluidity of the plasma membrane, we next examined the diffusional mobility of $DiIC_{16}$ and $DiIC_{18}$ under these conditions. Previous studies have established that changes in plasma membrane viscosity can be inferred from changes in the lateral mobility of these probes (32,39–42). For our studies, cells were either depleted of or loaded with cholesterol before $DiIC_{16}$ or $DiIC_{18}$ labeling as described in

TABLE 1 Semiquantitative analysis of plasma membrane cholesterol levels of COS-7 cells as assessed by filipin staining in response to various methods of cholesterol depletion and cholesterol loading

Condition	Control*	Treated*
Cholesterol depletion		
MβCD	100.0 ± 3.3 (66)	50.9 ± 2.9 (58)
O/N depletion	94.5 ± 5.7 (49)	82.4 ± 3.3 (58)
Cholesterol loading		
MβCD/chol	100.0 ± 3.3 (66)	307.5 ± 16.5 (58)
EtOH/chol	107.6 ± 4.0 (55)	146.0 ± 7.7 (64)

*Data were normalized to percent of control for MβCD-treated cells and are presented as mean ± SE (N) from three independent experiments. Note that the controls for the MβCD and MβCD/cholesterol samples are identical. Other controls were mock treated with carrier as described in Materials and Methods.

Materials and Methods. Somewhat surprisingly, MβCD treatment had little or no effect on either $DiIC_{16}$ or $DiIC_{18}$ diffusional mobility (Fig. 3). Both D and M_f for MβCD-treated cells were essentially identical to controls. In contrast, in cells loaded with cholesterol using MβCD/cholesterol complexes, D and M_f were each significantly decreased (Fig. 3). This effect was observed even when the cells had been previously cholesterol depleted using MβCD before loading (Fig. 3). These data suggest that membrane viscosity is increased by cholesterol loading using MβCD/cholesterol complexes but is essentially unaltered after the acute extraction of cholesterol with MβCD.

Acute cholesterol depletion and acute cholesterol loading both decrease the lateral mobility of Ras

We next asked how the diffusion of Ras was affected by acute cholesterol depletion or loading using MβCD. FRAP measurements showed that D for all three Ras isoforms was slowed in response to MβCD treatment (Fig. 4, *A–C*). The slowed D was accompanied by a small but statistically significant decrease in M_f in MβCD-treated cells (Fig. 4 *D*). Interestingly, the effect of MβCD treatment on D was more pronounced for GFP-KRas and GFP-HRas ($p < .0001$) than GFP-NRas ($p < .016$) when compared across multiple experiments (Fig. 4). This slowed diffusional mobility in MβCD-treated cells is similar to that observed for a variety of other plasma membrane proteins (12). However, as the slowing of protein diffusion was not accompanied by corresponding changes in fluorescent lipid diffusion (Fig. 3), the two likely occur by separate mechanisms (see below).

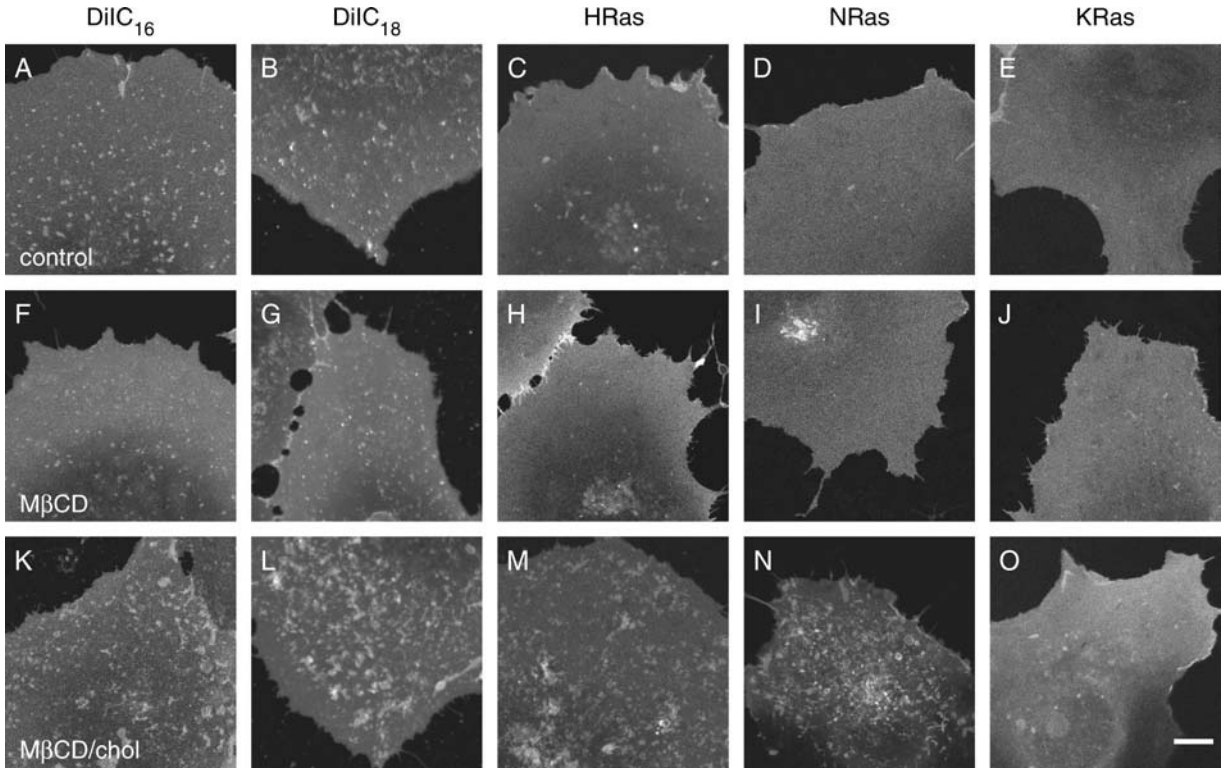

FIGURE 2 Distribution of fluorescent lipid probes and GFP-Ras isoforms in cholesterol-loaded and -depleted cells. Averaged prebleach images from confocal FRAP experiments showing the distribution of $DiIC_{16}$ (*A*, *F*, and *K*), $DiIC_{18}$ (*B*, *G*, and *L*), GFP-HRas (*C*, *H*, and *M*), GFP-NRas (*D*, *I*, and *N*), and GFP-KRas (*E*, *J*, and *O*) at the surface of COS-7 cells under control conditions (*A–E*), in cholesterol-depleted cells (*F–J*), and in cholesterol-loaded cells (*K–O*). At longer times after loading, larger KRas-positive structures were also occasionally observed in the perinuclear region (not shown). Bar, 10 μm.

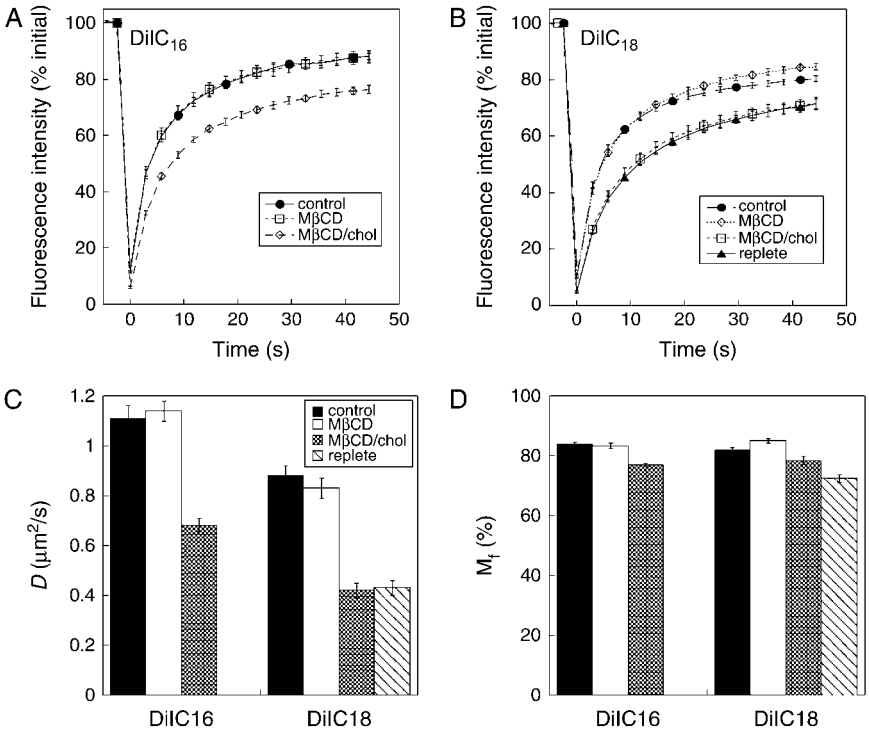

FIGURE 3 Effects of acute cholesterol depletion and cholesterol loading on the diffusional mobility of $DiIC_{16}$ and $DiIC_{18}$. (*A*) Recovery curves for $DiIC_{16}$ under control conditions (●), after cholesterol depletion with MβCD (□), or after cholesterol loading using MβCD/cholesterol complexes (◇). Data show the mean ± SE for 6–10 cells and are from a representative experiment ($N = 3$–5 independent experiments). (*B*) Recovery curves for $DiIC_{18}$ under control conditions (●), after cholesterol depletion with MβCD (◇), after treatment with MβCD/cholesterol complexes (□), or after treatment with MβCD followed by cholesterol repletion with MβCD/cholesterol complexes (▲). Data show the mean ± SE for 6–10 cells from a representative experiment ($N = 3$–5 independent experiments). (*C*) Mean D values for $DiIC_{16}$ and $DiIC_{18}$ diffusion in control (*solid bars*), MβCD-treated (*open bars*), MβCD/cholesterol-treated (*shaded bars*), and cholesterol-repleted (*striped bars*) cells. Data show the average from 2–3 independent experiments for a total of 20–50 cells. (*D*) Mean M_f values for $DiIC_{16}$ and $DiIC_{18}$ diffusion in (*solid bars*), MβCD-treated (*open bars*), MβCD/cholesterol-treated (*shaded bars*), and cholesterol-repleted (*striped bars*) cells. Data show the average from 2–3 independent experiments for a total of 20–50 cells.

Interestingly, cholesterol loading also led to significant slowing of Ras diffusion, and this effect was isoform specific. In particular, both D and M_f were decreased for GFP-HRas and GFP-NRas, whereas only D was decreased for GFP-KRas (Fig. 5). We considered the possibility that the accumulation of probe in vesicular structures in response to cholesterol loading (Fig. 2) could account for the source of the decreased M_f as these structures did not recover after FRAP measurements (Fig. 5, *A–D*). To test this, we performed experiments where we bleached the same region of interest twice in succession (12). M_f of GFP-HRas and GFP-NRas returned to control levels in the second measurement (Fig. 5, *E*, *F*, and *I*). This suggests that the loading-induced structures are not in rapid communication with the cell surface, consistent with the hypothesis that they form as the result of accelerated endocytosis (12,43). For GFP-KRas, which was excluded from these structures, M_f remained high in cholesterol-loaded cells and was unaltered in rebleach experiments (Fig. 5, *G* and *I*). In addition, we noted that D also increased as a result of the second bleach. Although the source of this effect is currently unknown, one possibility is that a pool of slowly diffusing proteins is eliminated by the first bleach.

Effects of other methods for cholesterol loading and depletion on plasma membrane cholesterol levels and the subcellular distribution of both Ras and $DiIC_{16}$

The observation that acute cholesterol depletion and loading both have similar effects on the diffusional mobility of Ras raises the possibility that this is mediated by the MβCD and

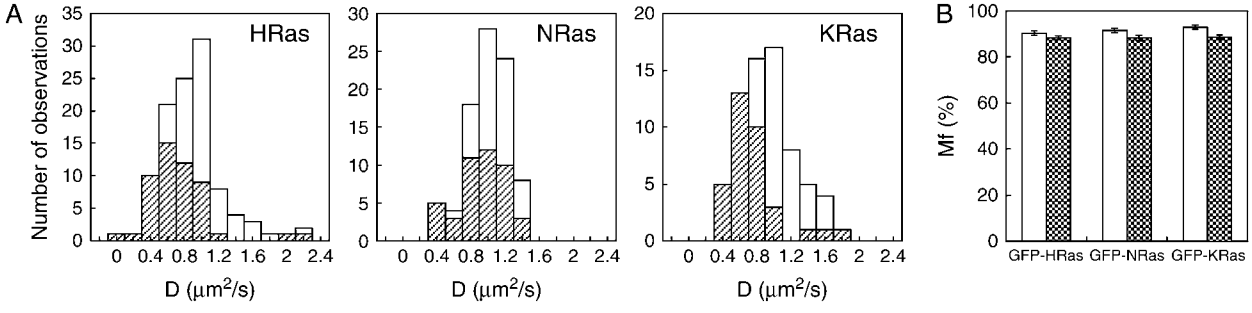

FIGURE 4 Acute cholesterol depletion with MβCD slows Ras diffusion. (*A*) Distribution of D in control (*open bars*) versus MβCD-treated cells (*shaded bars*) for GFP-HRas, GFP-NRas, and GFP-KRas. Data are pooled from 5–7 independent experiments for each protein. (*B*) Mean M_f for control (*open bars*) versus MβCD-treated cells (*shaded bars*) for GFP-HRas, GFP-NRas, and GFP-KRas.

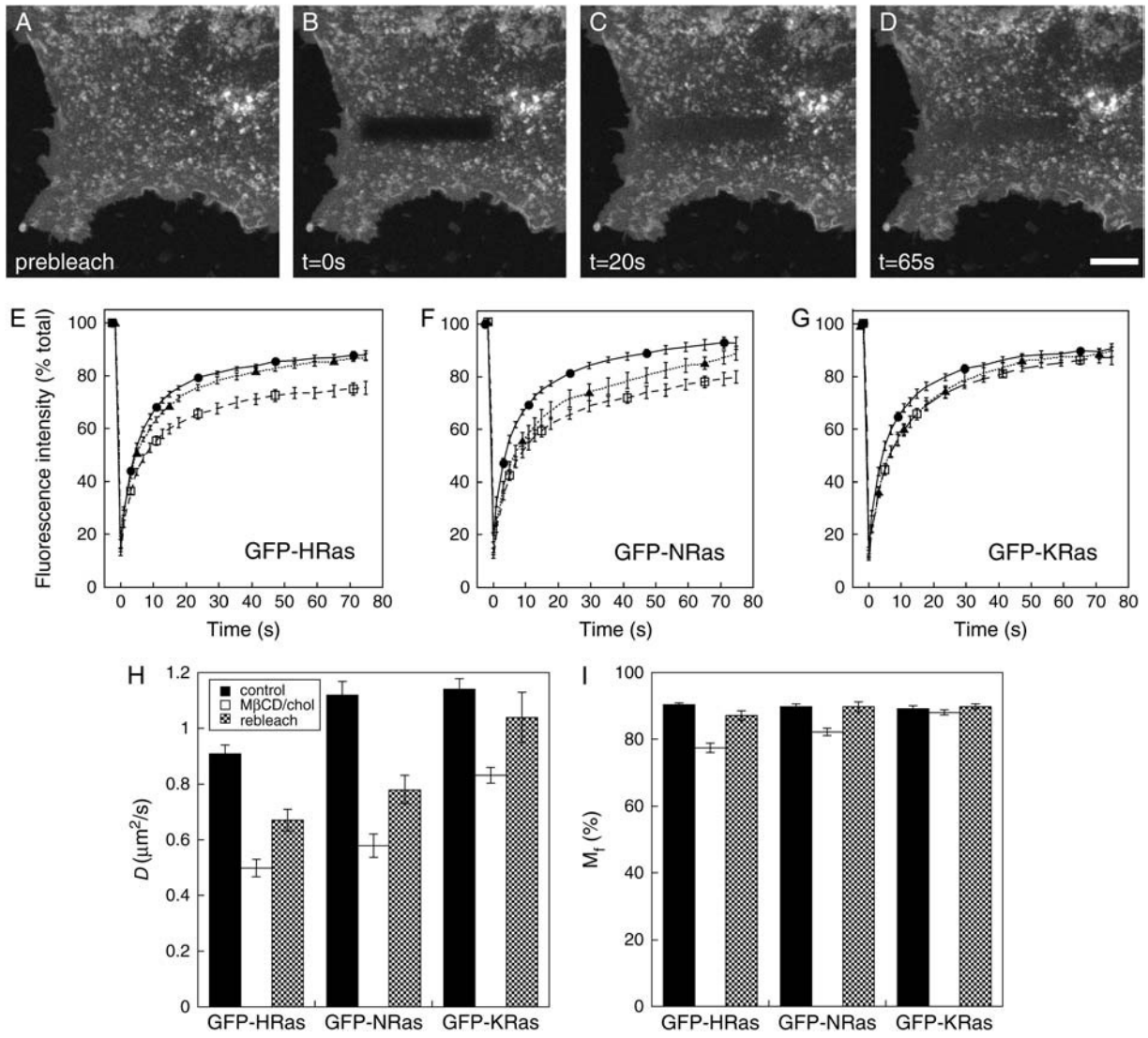

FIGURE 5 Acute cholesterol loading with MβCD/cholesterol complexes slows Ras diffusion. (*A–D*) Images from a FRAP experiment of cholesterol-loaded cells expressing GFP-HRas. Times after bleach are as indicated. Scale bar, 10 μm. (*E–G*) Mean fluorescence recovery curves for (*E*) GFP-HRas, (*F*) GFP-NRas, and (*G*) GFP-KRas under control conditions (●), in cholesterol-loaded cells (□), and after a second bleach of the same region of interest (ROI) in cholesterol-loaded cells (▲). Data are shown for a representative experiment ($N = 4–7$ cells). Data were collected at 1 s intervals; for clarity of presentation, not all data points are shown. Error bars, ± SE. (*H*) Mean D values for Ras diffusion under control conditions (*solid bars*), in cholesterol-loaded cells (*open bars*), and after a second bleach of the same ROI in cholesterol-loaded cells (*shaded bars*). Data are the average from 2–3 independent experiments for a total of 34–57 cells per protein. (*I*) Mean M_f values for Ras under control conditions (*solid bars*), in cholesterol-loaded cells (*open bars*), and after a second bleach of the same ROI in cholesterol-loaded cells (*shaded bars*). Data show the average from 2–3 independent experiments for a total of 34–57 cells per protein.

not changes in cholesterol levels per se. To test this possibility as well as to gain additional insight into how other methods for manipulating cholesterol levels alter the environment of the plasma membrane, we examined the effects of two additional depletion and loading paradigms. First, we performed cholesterol depletion by growing cells in lipoprotein-deficient serum in the presence of compactin plus mevalonate for 16 h (11,23). Under these conditions, cholesterol biosynthesis is inhibited and cells are simultaneously deprived of their source of exogenous cholesterol from serum. These conditions modestly decreased plasma membrane cholesterol levels as assessed by filipin staining (Table 1). As an additional method to add excess cholesterol, cells were incubated for 6 h with 25 μM cholesterol added from an ethanolic stock (23). This treatment slightly increased plasma membrane cholesterol levels (~1.5-fold over control values) as assessed by filipin staining (Table 1). Thus, both the depletion and incorporation of cholesterol into cells using these conditions was substantially less efficient than using MβCD as a carrier.

We next examined the effects of these treatments on cell morphology and the subcellular distribution of $DiIC_{16}$ and

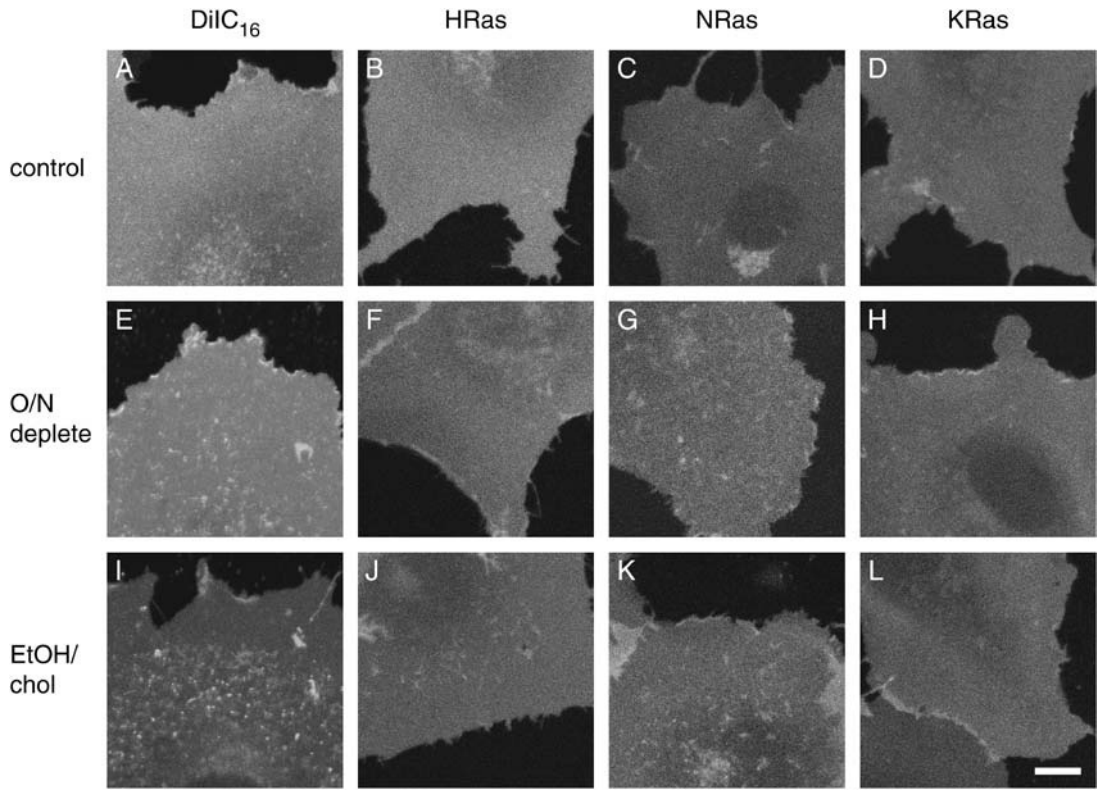

FIGURE 6 Distribution of fluorescent lipid probes and GFP-Ras isoforms in cells loaded or depleted of cholesterol using methods independent of MβCD. Averaged prebleach images from confocal FRAP experiments showing the distribution of $DiIC_{16}$ (*A*, *E*, and *I*), GFP-HRas (*B*, *F*, and *J*), GFP-NRas (*C*, *G*, and *K*), and GFP-KRas (*D*, *H*, and *L*) at the surface of COS-7 cells under control conditions (*A–D*), in cholesterol-depleted cells (*E–H*), and in cholesterol-loaded cells (*I–L*). Bar, 10 μm.

the three Ras isoforms (Fig. 6). The effects of overnight cholesterol depletion in LPDS plus compactin on cell morphology (Fig. 6, *E–H*) were much less pronounced than for MβCD-treated cells (Fig. 2, *F–J*). Cholesterol loading caused accumulation of plasma membrane markers in vesicular structures (Fig. 6, *I–L*) but to a lesser extent than observed for cells loaded with MβCD/cholesterol complexes (Fig. 2, *K–O*). The finding that two independent methods for cholesterol loading both lead to accumulation of these structures argues that this is the result of increased cholesterol and not a side effect of MβCD treatment.

Comparison of various methods of cholesterol loading and cholesterol depletion on $DiIC_{16}$ and Ras diffusional mobility and plasma membrane microviscosity

We performed FRAP experiments, directly comparing the effects of the two depletion and loading conditions to gain additional insight into whether they altered plasma membrane microenvironment in similar or distinct ways. These studies showed that the two depletion methods had distinctly different effects from one another. Although cholesterol depletion with MβCD had essentially no effect on $DiIC_{16}$ diffusion and slowed the diffusion of all three Ras isoforms, overnight incubation of cells with LPDS and compactin led to a small but reproducible increase in both lipid and Ras diffusion (Fig. 7, *A–D*). This effect was isoform specific, as the diffusional mobilities of GFP-HRas and GFP-NRas but not GFP-KRas were enhanced compared to control conditions (Fig. 7 *D*), consistent with a previous report (11).

As for the case of cholesterol loading with MβCD/cholesterol complexes, the addition of cholesterol via an ethanolic stock solution caused a slowing of both $DiIC_{16}$ and Ras diffusion (Fig. 7, *E–H*). Consistent with the observation that the EtOH/cholesterol treatment was less effective in delivering cholesterol to the membrane (Table 1), this treatment likewise had a smaller effect on diffusion than that achieved by loading with MβCD/cholesterol complexes.

Steady-state anisotropy measurements of membrane microviscosity as a function of cholesterol depletion and loading

To provide an independent assessment of the effects of various cholesterol depletion and loading conditions on plasma membrane viscosity, we performed measurements of TMA-DPH anisotropy, *r*. Previous studies using TMA-DPH

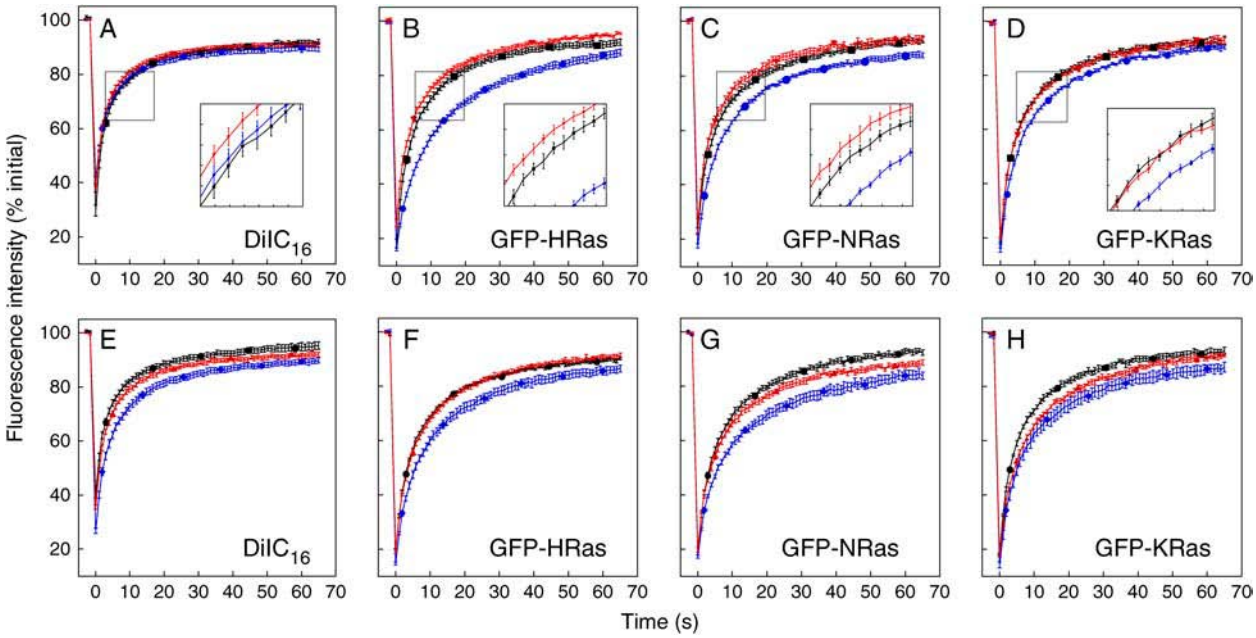

FIGURE 7 Comparison of the effects of different methods of cholesterol depletion and loading on the diffusional mobility of $DiIC_{16}$ and Ras. Recovery curves are shown for $DiIC_{16}$ (*A* and *E*), GFP-HRas (*B* and *F*), GFP-NRas (*C* and *G*), and GFP-KRas (*D* and *H*). (*A–D*) Cells were either mock depleted (*black squares*), cholesterol depleted using MβCD (*blue circles*), or depleted of cholesterol overnight (*red triangles*) as described in Materials and Methods before FRAP experiments. Insets show a closeup of the boxed regions. (*E–H*) Cells were either mock loaded (*black circles*), cholesterol loaded using MβCD/cholesterol complexes (*blue squares*), or loaded with cholesterol from an ethanol stock for 6 h (*red triangles*) as described in Materials and Methods before FRAP experiments. Recovery curves are representative of 3–4 independent experiments (mean ± SE).

or related probes have demonstrated that r is higher in model membranes in the liquid-ordered phase than in the liquid-disordered state (44–47). Furthermore, r is higher for detergent-resistant membrane (DRM) fractions than for bulk plasma membrane (45,46), and cholesterol depletion decreases r of both the plasma membrane (46,48) and DRMs (45,46). Interestingly, we found that depletion of cholesterol using MβCD had no effect on r, whereas r was significantly decreased in cells grown overnight in the presence of compactin and LPDS compared to cells treated with carrier alone (Table 2). Thus, the changes in r are consistent with the effects of the two cholesterol depletion methods on the lateral diffusion of $DiIC_{16}$ and $DiIC_{18}$, i.e., that MβCD treatment has essentially no effect on D, whereas a small increase in the halftime of recovery is observed in cells depleted overnight (Figs. 3 and 7). Furthermore, r was unchanged in response to cholesterol loading with either ethanol-solubilized cholesterol or MβCD/cholesterol complexes (Table 2), despite the decreased mobility of $DiIC_{16}$ under these conditions (Figs. 3 and 7). This suggests that plasma membrane microviscosity (reported by r) and macroviscosity (reported by D) are affected in different ways by the presence of supraphysiological levels of cholesterol.

TABLE 2 TMA-DPH anisotropy measurements in cholesterol-depleted and cholesterol-loaded cells

Condition	$r_{control}$	$r_{treated}$
Cholesterol depletion		
MβCD	0.170 ± .004 (116)	0.170 ± .004 (114)
O/N depletion	0.159 ± .005 (89)	0.127 ± .005 (90)**
Cholesterol loading		
MβCD/chol	0.170 ± .004 (116)	0.175 ± .004 (90)
EtOH/chol	0.179 ± .004 (60)	0.175 ± .005 (90)

Data show the mean ± SE from 3–4 independent experiments, consisting of 10 fields of cells per experiment. Data were collected for ROIs placed on the plasma membrane from three cells per field. Note that the controls for the MβCD and MβCD/cholesterol samples are identical. Other controls were mock treated with carrier as described in Materials and Methods.
**$p < .001$ compared to matched control, Student's t-test.

DISCUSSION

In this study, we examined the role of membrane viscosity in modulating the diffusional mobility of the small GTPase Ras. A resident of the cytoplasmic leaflet of the plasma membrane, Ras is known to diffuse extremely rapidly and exhibit very small immobile fractions, unlike the typical behavior of cell surface proteins. By altering plasma membrane cholesterol levels, we tested how the diffusional mobility of GFP-tagged versions of the three major Ras isoforms, HRas, NRas, and KRas, compares to that of the viscosity-sensitive fluorescent lipid probes $DiIC_{16}$ and $DiIC_{18}$ as measured by confocal FRAP in COS-7 cells. We found that all three Ras isoforms exhibit a lipid-like sensitivity to membrane viscosity. In cells loaded with excess cholesterol by two independent methods, Ras diffusion was slowed, paralleling the behavior of $DiIC_{16}$ and $DiIC_{18}$.

Interestingly, whereas overnight cholesterol depletion increased both Ras and $DiIC_{16}$ mobilities, acute cholesterol depletion using MβCD, which under the conditions of our experiments had no detectable effect on D for either $DiIC_{16}$ or $DiIC_{18}$, significantly decreased D for all three Ras isoforms. This indicates that the effects of cholesterol depletion on protein and lipid diffusion in cell membranes are highly dependent on the depletion method used.

Effects of cholesterol depletion on protein and lipid diffusion at the cell surface

The relationship between membrane cholesterol content, the diffusional mobility of lipid probes, and membrane viscosity has long been recognized (39–41). More recently, the dependence of lateral mobility of both proteins and lipids on cellular cholesterol levels has been revisited in the context of the lipid raft model. Strikingly, the reported effects of cholesterol depletion on protein and lipid diffusion at the cell surface vary widely. In several cases, D of either proteins or lipids has been shown to drop in response to cholesterol depletion (12,19,34,49,50). For example, in CHO cells, D for $DiIC_{16}$, $DiIC_{18,}$ and two forms of Class II Major Histocompatibility Complex (MHC-II) differing in their membrane anchor were substantially slowed after cholesterol depletion with MβCD, an effect that was reversed by cholesterol repletion for MHC-II (49). Reversibly slowed diffusion of $DiIC_{16}$ and $DiIC_{18}$ in response to cholesterol depletion has also been observed in RBL and HEK cells (34). Edidin and co-workers observed immobilization of HLA-I protein diffusion after cholesterol depletion in several different cell types; however, this effect was primarily apparent as a decrease in M_f and was not reversed by cholesterol repletion (51). Furthermore, we found that MβCD treatment led to a twofold drop in D for all proteins examined, regardless of whether they are raft associated (12). Yet, in other instances, protein diffusional mobility (including HRas) was found to increase in cholesterol-depleted cells (11,27,52,53).

Our results provide at least a partial explanation for some of the source of otherwise apparently contradictory findings. First, we show that cholesterol depletion does not necessarily have the same effects on protein and lipid diffusion. For example, MβCD treatment, which significantly slowed the diffusion of a wide range of plasma membrane proteins (12), had little to no effect on $DiIC_{16}$ or $DiIC_{18}$ diffusion (Fig. 3, Table 3). This lack of effect of cholesterol depletion on lipid probe diffusion is not without precedent, as early studies of cholesterol-depleted erythrocytes reached a similar conclusion for measurements made at physiological temperatures (54). Secondly, we find that the effects of cholesterol depletion on lipid diffusion are not necessarily correlated with changes in membrane microviscosity as reported by TMA-DPH anisotropy. Although acute MβCD extraction caused a more significant loss of cholesterol from the cell surface and slowing of DiI diffusion than did overnight cholesterol depletion, only overnight depletion lead to a detectable drop in r (Table 3). This could indicate that more substantial changes in membrane viscosity occur in response to overnight cholesterol depletion. Alternatively, decreased viscosity is not detected in MβCD-treated cells due to competing effects causing membrane stiffening (see below). Finally, we find that the consequences of cholesterol depletion are strongly dependent on the method used: MβCD slows Ras diffusion, whereas growth of cells in the presence of LPDS and compactin slightly increases it. Given the central role that cholesterol depletion currently plays in studies of lipid raft structure and function, it will be important to further dissect how cells sense and respond to each of these treatments in future studies.

TABLE 3 Summary of the effects of cholesterol depletion and cholesterol loading on plasma membrane cholesterol levels; diffusional mobility of Ras, fluorescent lipid probes, and GPI-anchored proteins; and membrane microviscosity

Condition	[Chol]	D_{DiIC16}	D_{Ras}	D_{GPI}*	r
Cholesterol depletion					
MβCD	↓↓	unchanged	↓↓	↓↓↓	unchanged
O/N depletion	↓	↑	↑	n.d.	↓
Cholesterol loading					
MβCD/chol	↑↑↑	↓↓	↓↓	unchanged	unchanged
EtOH/chol	↑	↓	↓	n.d.	unchanged

n.d., not determined.
*From (12).

Additional factors are also likely to contribute to the varied effects of cholesterol depletion on protein and lipid diffusion in cells. The balance of liquid-ordered/liquid-disordered domains may differ significantly between cell types, causing some to be more sensitive to small changes in cholesterol levels than others. In this regard it is important to note that in simple lipid mixtures, the dependence of lipid probe diffusion on cholesterol is a strong function of the lipid phase (liquid ordered versus liquid disordered) as well as the absolute cholesterol concentration. Typically, cholesterol is thought to increase the fluidity of gel-preferring lipids and decrease the fluidity within a liquid-disordered environment. However, over intermediate ranges of cholesterol levels, D has been shown to be relatively insensitive to cholesterol content within a liquid-disordered phase (32,55). In a ternary mixture producing a coexisting liquid-ordered and liquid-disordered phases, lipid probe mobility increased as a function of increased cholesterol, then slowed down as cholesterol concentrations were further increased to a point where phase separation was no longer observed (32). Clearly, even in such model systems D has the potential to increase, decrease, or remain unchanged in response to changing cholesterol levels.

Cholesterol-dependent signaling pathways are another mechanism that is likely to influence the membrane environment experienced by membrane proteins and lipids by

causing changes in membrane structure and composition secondary to the effects of cholesterol depletion on membrane cholesterol levels per se. One such recently identified pathway appears to result in stabilization of the actin cytoskeleton (51). This mechanism is further supported by a recent report of increased membrane stiffening in cholesterol-depleted aortic endothelial cells (56). The presence of cholesterol/phospholipid complexes could also be important in regulating membrane viscosity. For example, cholesterol depletion could potentially eliminate cholesterol-phospholipid complexes, leaving behind solidlike phospholipids (57). Finally, long-term cholesterol depletion could initiate compensatory changes in membrane lipid composition. It will be interesting to determine if these differences are reflected in the organization and function of lipid rafts and related membrane microdomains as assessed by other functional and structural criteria.

Effects of cholesterol loading on protein and lipid diffusion at the cell surface

Our findings provide several new insights into the physiological consequences of excess cholesterol on the environment experienced by plasma membrane proteins and lipids. One major result is the decreased D and M_f observed for fluorescent lipid probes in cholesterol-loaded cells. The effect on D can be explained by an increase in membrane viscosity, whereas the effects on M_f likely are the result of the accelerated accumulation of the probes in response to cholesterol loading (see below). Although we observed qualitatively similar effects of both loading conditions tested, loading with MβCD/cholesterol complexes had a larger effect on diffusional mobilities (Fig. 7), likely the result of its more efficient delivery of cholesterol to the plasma membrane (Table 1). Importantly, the changes in membrane environment reported by $DiIC_{16}$ and $DiIC_{18}$ in response to cholesterol loading were likewise sensed by Ras diffusion. This property is unique to Ras, as two previous studies showed that the diffusional mobility of GPI-anchored and transmembrane proteins were insensitive to cholesterol loading (12,49). We hypothesize that for most proteins, other features of the membrane are more important than viscosity, contributing to their overall slow diffusion compared to Ras (12,58). Despite the significant drop in D for $DiIC_{16}$ and Ras in cholesterol-loaded cells, TMA-DPH anisotropy measurements revealed no detectable change in plasma membrane microviscosity under these conditions. This is reminiscent of the finding that the fluidity of red blood cell membranes is constant at supraphysiological cholesterol:phospholipid ratios (59). Our results also provide further support to the hypothesis that excess cholesterol accelerates endocytosis (12,43), as we observed a substantial increase in the intracellular accumulation of HRas, NRas, $DiIC_{16}$, and $DiIC_{18}$ in cholesterol-loaded cells (Figs. 2 and 6) that led to a corresponding decreased M_f (Figs. 3 and 7). Exactly how cholesterol levels modulate the cell's endocytic machinery remains to be determined.

Implications of the isoform-specific behavior of Ras

Current models suggest that HRas resides in lipid rafts and shifts to a nonraft environment upon activation and that KRas resides in nonraft domains in both its GTP- and GDP-bound forms (11,15–18). Our results provide several lines of support for this model. In agreement with a recent report (11), KRas diffusion was unaffected by overnight cholesterol depletion, whereas the diffusion of both HRas and NRas were slightly increased under these conditions (Fig. 7). Unlike GFP-HRas and GFP-NRas, GFP-KRas was excluded from intracellular structures in cholesterol-loaded cells (Fig. 2). This suggests that KRas either does not undergo endocytosis or that it rapidly diffuses back to the plasma membrane after internalization, consistent with a recent study (60). Moreover, KRas diffusion was slowed by cholesterol loading to a lesser extent than that of HRas or NRas (Fig. 5), suggesting it resides in a more cholesterol-poor environment. Since the diffusion of both raft (HRas, NRas) and nonraft (KRas) preferring forms of Ras were slowed in the presence of excess cholesterol, these results also imply that cholesterol is incorporated into both environments and does not act simply to increase the surface coverage of raftlike domains.

The preferred microdomain localization of NRas has been less well studied than for either HRas or KRas, but at least one study suggests that NRas, like HRas, is predominantly raft associated (18). Our data imply that either the extent of partitioning of NRas or its microenvironment is distinct from that of HRas. In particular, we observed that even though the diffusional mobility of H-, N-, and KRas were comparable under steady-state conditions (Fig. 1), D for NRas was less affected by cholesterol depletion with MβCD than for either HRas or KRas (Fig. 4). This suggests that of the three major Ras isoforms, in this regard, NRas is the most lipidlike in its behavior.

Membrane environment experienced by proteins localized to the inner leaflet

We propose that fast and relatively unconfined diffusion exhibited by Ras may represent a general feature of lipid-anchored proteins residing on the inner leaflet of the plasma membrane. This rapid diffusion may be potentiated by the lipid environment of the inner leaflet, which is thought to be less viscous than the outer leaflet (61–64). This could explain why Ras diffusion is even faster than that of GPI-anchored proteins, which have long been recognized for their high lateral mobility (65–68). Our initial measurements indicate that GFP-Fyn, a myristoylated and palmitoylated inner leaflet protein, also diffuses as fast as or faster than GPI-anchored proteins, albeit at a somewhat reduced rate com-

pared to Ras (12). It remains to be determined if this difference is due to the nature of the membrane anchors or specific protein-based interactions.

It is interesting to note that despite its overall fast diffusion, Ras retains the ability to sense barriers to diffusion induced by MβCD treatment that are also experienced by transmembrane, GPI-anchored, and glycolipid-binding proteins (12). However, Ras diffusion is impacted to a lesser extent than other proteins. In particular, D was slowed 30% for GFP-KRas and GFP-HRas and 12% for GFP-NRas relative to control cells (Fig. 5) in comparison to an average 50% decrease observed for transmembrane, GPI-anchored, and glycolipid-binding proteins under identical depletion conditions (12). These data imply that Ras does not completely escape the barriers to diffusion sensed by other proteins but does appear to experience them to a lesser degree. Thus, despite its lipid anchor, Ras diffusion is not completely analogous to that of a lipid molecule.

Possible physiological consequences of viscosity-limited protein diffusion

We hypothesize that the ability of Ras to sense membrane viscosity may allow for a unique regulation of protein mobility and localization by membrane microdomains. Ras signaling is postulated to occur in both raft and nonraft regions of the membrane depending on the specific isoform studied (11,15,17). Lipid rafts are often proposed to correspond to regions of confined and/or slowed diffusion (10,12,69–72). Membrane viscosity could provide a potential mechanism for slowing protein diffusion within rafts. Lipid diffusion is typically two- to threefold lower in the liquid-ordered raft phase than in disordered membrane in model systems (42,73) although even larger differences have recently been reported (32). Since in cell membranes the mobility of most proteins is below the viscosity-induced limit (2,3), it seems unlikely that rafts could slow diffusion by a viscosity-mediated mechanism in vivo. Indeed, we previously showed that the long-range diffusion of most raft proteins is dominated by factors other than their association with rafts (12). However, the ability of Ras diffusion to respond to local membrane viscosity could provide a novel mechanism for regulating its interactions with membrane microdomains. This could potentially explain why despite the rapid diffusion of Ras, its association with microdomains is sufficiently stable to allow for detection of these domains by electron microscopy (16). Recent observations that membrane viscosity helps regulate events such as cell motility (50,74) further highlight the possibility that such behavior may have significant functional consequences for cells.

We are grateful to Glenn Hendrix for expert technical assistance at early stages of this work, Carl Rogers for help with data analysis, Mark Philips for providing the GFP-Ras constructs, and Harden McConnell and Marija Vrljic for sharing results before publication. We also thank Alyssa Hasty for assistance with the preparation of lipoprotein-depleted serum, Jon Rocheleau and Mark Rizzo for guidance in setting up the anisotropy measurements, and our colleagues Audi Byrne, Mingming Hao, Dave Piston, and Al Beth for comments on an earlier version of the manuscript.

REFERENCES

1. Saffman, P. G., and M. Delbrück. 1975. Brownian motion in biological membranes. *Proc. Natl. Acad. Sci. USA*. 72:3111–3113.
2. Jacobson, K., A. Ishihara, and R. Inman. 1987. Lateral diffusion of proteins in membranes. *Annu. Rev. Physiol*. 49:163–175.
3. Edidin, M. 1996. Getting there is only half the fun. *Curr. Top. Membr*. 43:1–13.
4. Edidin, M. 2001. Shrinking patches and slippery rafts: scales of domains in the plasma membrane. *Trends Cell Biol*. 11:492–496.
5. Kusumi, A., and Y. Sako. 1996. Cell surface organization by the membrane skeleton. *Curr. Opin. Cell Biol*. 8:566–574.
6. Saxton, M. J., and K. Jacobson. 1997. Single-particle tracking: applications to membrane dynamics. *Annu. Rev. Biophys. Biomol. Struct*. 26:373–399.
7. Casey, P. J. 1995. Protein lipidation in cell signaling. *Science*. 268: 221–225.
8. Edidin, M., M. C. Zuniga, and M. P. Sheetz. 1994. Truncation mutants define and locate cytoplasmic barriers to lateral mobility of membrane glycoproteins. *Proc. Natl. Acad. Sci. USA*. 91:3378–3382.
9. Fujiwara, T., K. Ritchie, H. Murakoshi, K. Jacobson, and A. Kusumi. 2002. Phospholipids undergo hop diffusion in compartmentalized cell membrane. *J. Cell Biol*. 157:1071–1081.
10. Niv, H., O. Gutman, Y. I. Henis, and Y. Kloog. 1999. Membrane interactions of a constitutively active GFP-Ki-Kas 4B and their role in signaling. Evidence from lateral mobility studies. *J. Biol. Chem*. 274: 1606–1613.
11. Niv, H., O. Gutman, Y. Kloog, and Y. I. Henis. 2002. Activated K-Ras and H-Ras display different interactions with saturable nonraft sites at the surface of live cells. *J. Cell Biol*. 157:865–872.
12. Kenworthy, A. K., B. J. Nichols, C. L. Remmert, G. M. Hendrix, M. Kumar, J. Zimmerberg, and J. Lippincott-Schwartz. 2004. Dynamics of putative raft-associated proteins at the cell surface. *J. Cell Biol*. 165: 735–746.
13. Silvius, J. R. 2002. Mechanisms of Ras protein targeting in mammalian cells. *J. Membr. Biol*. 190:83–92.
14. Hancock, J. F. 2003. Ras proteins: different signals from different locations. *Nat. Rev. Mol. Cell Biol*. 4:373–384.
15. Prior, I. A., A. Harding, J. Yan, J. Sluimer, R. G. Parton, and J. F. Hancock. 2001. GTP-dependent segregation of H-ras from lipid rafts is required for biological activity. *Nat. Cell Biol*. 3:368–375.
16. Prior, I. A., C. Muncke, R. G. Parton, and J. F. Hancock. 2003. Direct visualization of Ras proteins in spatially distinct cell surface microdomains. *J. Cell Biol*. 160:165–170.
17. Matallanas, D., I. Arozarena, M. T. Berciano, D. S. Aaronson, A. Pellicer, M. Lafarga, and P. Crespo. 2003. Differences on the inhibitory specificities of H-Ras, K-Ras, and N-Ras (N17) dominant negative mutants are related to their membrane microlocalization. *J. Biol. Chem*. 278:4572–4581.
18. Kranenburg, O., I. Verlaan, and W. H. Moolenaar. 2001. Regulating c-Ras function: cholesterol depletion affects caveolin association, GTP loading, and signaling. *Curr. Biol*. 11:1880–1884.
19. Lommerse, P. H., G. A. Blab, L. Cognet, G. S. Harms, B. E. Snaar-Jagalska, H. P. Spaink, and T. Schmidt. 2004. Single-molecule imaging of the H-ras membrane-anchor reveals domains in the cytoplasmic leaflet of the cell membrane. *Biophys. J*. 86:609–616.
20. Murakoshi, H., R. Iino, T. Kobayashi, T. Fujiwara, C. Ohshima, A. Yoshimura, and A. Kusumi. 2004. Single-molecule imaging analysis of Ras activation in living cells. *Proc. Natl. Acad. Sci. USA*. 101:7317–7322.

21. Choy, E., V. K. Chiu, J. Silletti, M. Feoktistov, T. Morimoto, D. Michaelson, I. E. Ivanov, and M. R. Philips. 1999. Endomembrane trafficking of Ras: the CAAX motif targets proteins to the ER and Golgi. *Cell*. 98:69–80.

22. Mayor, S., S. Sabharanjak, and F. R. Maxfield. 1998. Cholesterol-dependent retention of GPI-anchored proteins in endosomes. *EMBO J*. 17:4626–4638.

23. Adams, C. M., J. Reitz, J. K. De Brabander, J. D. Feramisco, L. Li, M. S. Brown, and J. L. Goldstein. 2004. Cholesterol and 25-hydroxycholesterol inhibit activation of SREBPs by different mechanisms, both involving SCAP and Insigs. *J. Biol. Chem.* 279:52772–52780.

24. Siggia, E. D., J. Lippincott-Schwartz, and S. Bekiranov. 2000. Diffusion in inhomogeneous media: theory and simulations applied to whole cell photobleach recovery. *Biophys. J*. 79:1761–1770.

25. Ellenberg, J., E. D. Siggia, J. E. Moreira, C. L. Smith, J. F. Presley, H. J. Worman, and J. Lippincott-Schwartz. 1997. Nuclear membrane dynamics and reassembly in living cells: targeting of an inner nuclear membrane protein in interphase and mitosis. *J. Cell Biol*. 138:1193–1206.

26. Weiss, M. 2004. Challenges and artifacts in quantitative photobleaching experiments. *Traffic*. 5:662–671.

27. Rotblat, B., I. A. Prior, C. Muncke, R. G. Parton, Y. Kloog, Y. I. Henis, and J. F. Hancock. 2004. Three separable domains regulate GTP-dependent association of H-ras with the plasma membrane. *Mol. Cell. Biol*. 24:6799–6810.

28. Wu, Y., F. F. Sun, D. M. Tong, and B. M. Taylor. 1996. Changes in membrane properties during energy depletion-induced cell injury studied with fluorescence microscopy. *Biophys. J*. 71:91–100.

29. Rocheleau, J. V., M. Edidin, and D. W. Piston. 2003. Intrasequence GFP in class I MHC molecules, a rigid probe for fluorescence anisotropy measurements of the membrane environment. *Biophys. J*. 84:4078–4086.

30. Axelrod, D. 1979. Carbocyanine dye orientation in red cell membrane studied by microscopic fluorescence polarization. *Biophys. J*. 26:557–573.

31. Klausner, R. D., and D. E. Wolf. 1980. Selectivity of fluorescent lipid analogues for lipid domains. *Biochemistry*. 19:6199–6203.

32. Kahya, N., D. Scherfeld, K. Bacia, B. Poolman, and P. Schwille. 2003. Probing lipid mobility of raft-exhibiting model membranes by fluorescence correlation spectroscopy. *J. Biol. Chem*. 278:28109–28115.

33. Hao, M., S. Mukherjee, and F. R. Maxfield. 2001. Cholesterol depletion induces large scale domain segregation in living cell membranes. *Proc. Natl. Acad. Sci. USA*. 98:13072–13077.

34. Bacia, K., D. Scherfeld, N. Kahya, and P. Schwille. 2004. Fluorescence correlation spectroscopy relates rafts in model and native membranes. *Biophys. J*. 87:1034–1043.

35. Parton, R. G., and J. F. Hancock. 2004. Lipid rafts and plasma membrane microorganization: insights from Ras. *Trends Cell Biol*. 14: 141–147.

36. Christian, A. E., M. P. Haynes, M. C. Phillips, and G. H. Rothblat. 1997. Use of cyclodextrins for manipulating cellular cholesterol content. *J. Lipid Res*. 38:2264–2272.

37. Feng, B., P. M. Yao, Y. Li, C. M. Devlin, D. Zhang, H. P. Harding, M. Sweeney, J. X. Rong, G. Kuriakose, E. A. Fisher, A. R. Marks, D. Ron, and I. Tabas. 2003. The endoplasmic reticulum is the site of cholesterol-induced cytotoxicity in macrophages. *Nat. Cell Biol*. 5:781–792.

38. Simons, K., and D. Toomre. 2000. Lipid rafts and signal transduction. *Nat. Rev. Mol. Cell Biol*. 1:31–41.

39. Searls, D. B., and M. Edidin. 1981. Lipid composition and lateral diffusion in plasma membranes of teratocarcinoma-derived cell lines. *Cell*. 24:511–517.

40. Schootemeijer, A., G. Gorter, L. G. Tertoolen, S. W. De Laat, and J. W. Akkerman. 1995. Relation between membrane fluidity and signal transduction in the human megakaryoblastic cell line MEG-01. *Biochim. Biophys. Acta*. 1236:128–134.

41. Bloom, J. A., and W. W. Webb. 1983. Lipid diffusibility in the intact erythrocyte membrane. *Biophys. J*. 42:295–305.

42. Dietrich, C., L. A. Bagatolli, Z. N. Volovyk, N. L. Thompson, M. Levi, K. Jacobson, and E. Gratton. 2001a. Lipid rafts reconstituted in model systems. *Biophys. J*. 80:1417–1428.

43. Sharma, D. K., J. C. Brown, A. Choudhury, T. E. Peterson, E. Holicky, D. L. Marks, R. Simari, R. G. Parton, and R. E. Pagano. 2004. Selective stimulation of caveolar endocytosis by glycosphingolipids and cholesterol. *Mol. Biol. Cell*. 15:3114–3122.

44. Schroeder, R., E. London, and D. Brown. 1994. Interactions between saturated acyl chains confer detergent resistance on lipids and glycosylphosphatidylinositol (GPI)-anchored proteins: GPI-anchored proteins in liposomes and cells show similar behavior. *Proc. Natl. Acad. Sci. USA*. 91:12130–12134.

45. Gidwani, A., D. Holowka, and B. Baird. 2001. Fluorescence anisotropy measurements of lipid order in plasma membranes and lipid rafts from RBL-2H3 mast cells. *Biochemistry*. 40:12422–12429.

46. Sinha, M., S. Mishra, and P. G. Joshi. 2003. Liquid-ordered microdomains in lipid rafts and plasma membrane of U-87 MG cells: a time-resolved fluorescence study. *Eur. Biophys. J*. 32:381–391.

47. Wang, J., Megha, and E. London. 2004. Relationship between sterol/steroid structure and participation in ordered lipid domains (lipid rafts): implications for lipid raft structure and function. *Biochemistry*. 43: 1010–1018.

48. Hannan, L. A., and M. Edidin. 1996. Traffic, polarity, and detergent solubility of a glycosylphosphatidylinositol-anchored protein after LDL-deprivation of MDCK cells. *J. Cell Biol*. 133:1265–1276.

49. Vrljic, M., S. Y. Nishimura, W. E. Moerner, and H. M. McConnell. 2005. Cholesterol depletion suppresses the translational diffusion of class II major histocompatibility complex proteins in the plasma membrane. *Biophys. J*. 88:334–347.

50. Vasanji, A., P. K. Ghosh, L. M. Graham, S. J. Eppell, and P. L. Fox. 2004. Polarization of plasma membrane microviscosity during endothelial cell migration. *Dev. Cell*. 6:29–41.

51. Kwik, J., S. Boyle, D. Fooksman, L. Margolis, M. P. Sheetz, and M. Edidin. 2003. Membrane cholesterol, lateral mobility, and the phosphatidylinositol 4,5-bisphosphate-dependent organization of cell actin. *Proc. Natl. Acad. Sci. USA*. 100:13964–13969.

52. Pralle, A., P. Keller, E. L. Florin, K. Simons, and J. K. Horber. 2000. Sphingolipid-cholesterol rafts diffuse as small entities in the plasma membrane of mammalian cells. *J. Cell Biol*. 148:997–1008.

53. Shvartsman, D. E., M. Kotler, R. D. Tall, M. G. Roth, and Y. I. Henis. 2003. Differently anchored influenza hemagglutinin mutants display distinct interaction dynamics with mutual rafts. *J. Cell Biol*. 163:879–888.

54. Thompson, N. L., and D. Axelrod. 1980. Reduced lateral mobility of a fluorescent lipid probe in cholesterol-depleted erythrocyte membrane. *Biochim. Biophys. Acta*. 597:155–165.

55. Almeida, P. F., W. L. Vaz, and T. E. Thompson. 1992. Lateral diffusion in the liquid phases of dimyristoylphosphatidylcholine/cholesterol lipid bilayers: a free volume analysis. *Biochemistry*. 31:6739–6747.

56. Byfield, F. J., H. Aranda-Espinoza, V. G. Romanenko, G. H. Rothblat, and I. Levitan. 2004. Cholesterol depletion increases membrane stiffness of aortic endothelial cells. *Biophys. J*. 87:3336–3343.

57. Vrljic, M., S. Y. Nishimura, S. Brasselet, W. E. Moerner, and H. M. McConnell. 2002. Translational diffusion of individual Class II MHC membrane proteins in cells. *Biophys. J*. 83:2681–2692.

58. Lagerholm, B. C., G. E. Weinreb, K. Jacobson, and N. L. Thompson. 2005. Detecting microdomains in intact cell membranes. *Annu. Rev. Phys. Chem*. 56:309–336.

59. Cooper, R. A. 1978. Influence of increased membrane cholesterol on membrane fluidity and cell function in human red blood cells. *J. Supramol. Struct*. 8:413–430.

60. Roy, S., B. Wyse, and J. F. Hancock. 2002. H-Ras signaling and K-Ras signaling are differentially dependent on endocytosis. *Mol. Cell. Biol.* 22:5128–5140.

61. Julien, M., J. F. Tournier, and J. F. Tocanne. 1993. Differences in the transbilayer and lateral motions of fluorescent analogs of phosphatidylcholine and phosphatidylethanolamine in the apical plasma membrane of bovine aortic endothelial cells. *Exp. Cell Res.* 208:387–397.

62. Morrot, G., S. Cribier, P. F. Devaux, D. Geldwerth, J. Davoust, J. F. Bureau, P. Fellmann, P. Herve, and B. Frilley. 1986. Asymmetric lateral mobility of phospholipids in the human erythrocyte membrane. *Proc. Natl. Acad. Sci. USA.* 83:6863–6867.

63. el Hage Chahine, J. M., S. Cribier, and P. F. Devaux. 1993. Phospholipid transmembrane domains and lateral diffusion in fibroblasts. *Proc. Natl. Acad. Sci. USA.* 90:447–451.

64. Devaux, P. F., and R. Morris. 2004. Transmembrane asymmetry and lateral domains in biological membranes. *Traffic.* 5:241–246.

65. Zhang, F., B. Crise, B. Su, Y. Hou, J. K. Rose, A. Bothwell, and K. Jacobson. 1991. Lateral diffusion of membrane-spanning and glycosylphosphatidylinositol-linked proteins: toward establishing rules governing the lateral mobility of membrane proteins. *J. Cell Biol.* 115:75–84.

66. Edidin, M., and I. Stroynowski. 1991. Differences between the lateral organization of conventional and inositol phospholipid-anchored membrane proteins. A further definition of micrometer scale membrane domains. *J. Cell Biol.* 112:1143–1150.

67. Ishihara, A., Y. Hou, and K. Jacobson. 1987. The Thy-1 antigen exhibits rapid lateral diffusion in the plasma membrane of rodent lymphoid cells and fibroblasts. *Proc. Natl. Acad. Sci. USA.* 84:1290–1293.

68. Noda, M., K. Yoon, G. A. Rodan, and D. E. Koppel. 1987. High lateral mobility of endogenous and transfected alkaline phosphatase: a phosphatidylinositol-anchored membrane protein. *J. Cell Biol.* 105:1671–1677.

69. Dietrich, C., B. Yang, T. Fujiwara, A. Kusumi, and K. Jacobson. 2002. Relationship of lipid rafts to transient confinement zones detected by single particle tracking. *Biophys. J.* 82:274–284.

70. Kusumi, A., I. Koyama-Honda, and K. Suzuki. 2004. Molecular dynamics and interactions for creation of stimulation-induced stabilized rafts from small unstable steady-state rafts. *Traffic.* 5:213–230.

71. Anderson, R. G. W., and K. Jacobson. 2002. A role for lipid shells in targeting proteins to caveolae, rafts and other lipid domains. *Science.* 296:1821–1825.

72. Jacobson, K., and C. Dietrich. 1999. Looking at lipid rafts? *Trends Cell Biol.* 9:87–91.

73. Almeida, P. F., W. L. Vaz, and T. E. Thompson. 1993. Percolation and diffusion in three-component lipid bilayers: effect of cholesterol on an equimolar mixture of two phosphatidylcholines. *Biophys. J.* 64:399–412.

74. Ghosh, P. K., A. Vasanji, G. Murugesan, S. J. Eppell, L. M. Graham, and P. L. Fox. 2002. Membrane microviscosity regulates endothelial cell motility. *Nat. Cell Biol.* 4:894–900.